Frontiers in Bioscience Landmark

Front. Biosci. (Landmark Ed) **2025**; 30(3): 26045
https://doi.org/10.31083/FBL26045

Original Research

Effect of HepG2-Derived Exosome with PDGF-D Knockdown on Transformation of Normal Fibroblasts into Tumor-Associated Fibroblasts in Liver Cancer

Yan-Yan Wu[1], Liu-Shen-Yan Yu[1], Han-Yu Zhou[1], Jun-Chao Xue[1,*]

[1]Department of Pharmacy, Tongde Hospital of Zhejiang Province, 310012 Hangzhou, Zhejiang, China
*Correspondence: samxer@163.com (Jun-Chao Xue)
Academic Editor: Amancio Carnero Moya
Submitted: 7 August 2024 Revised: 12 September 2024 Accepted: 26 September 2024 Published: 21 March 2025

Abstract

Background: It is known that the transformation of liver cancer-mediated fibroblasts into cancer-related fibroblasts (CAFs) is beneficial to the development of liver cancer. However, the specific mechanism is still unclear. **Methods**: Human hepatocarcinoma (HepG2) cells were treated with short hairpin RNA (shRNA) of platelet-derived growth factor-D (shPDGF-D) vector, and the exosomes secreted by the cells were separated using ultracentrifugation and identified by using nanoparticle tracking analysis, transmission electron microscope, and western blot analysis. Exosomes were co-cultured with mouse primary fibroblasts, and then the activity, proliferation, cell cycle, migration, epithelial-mesenchymal transition- (EMT-) and CAF marker-related protein expression levels of fibroblasts were determined by cell counting kit-8 (CCK-8), immunofluorescence, flow cytometry, wound healing, real-time reverse transcription-PCR, and western blotting assays, respectively. Co-cultured fibroblasts were mixed with HepG2 cells and injected subcutaneously into mice to construct animal models. The size and weight of xenograft tumor and the expression of epithelial-mesenchymal transition- (EMT-), angiogenesis- and CAFs marker-related proteins were detected. **Results**: The exosomes inhibited the proliferation, migration, EMT, and induced cell cycle arrest, as well as decreased the expression of α-*SMA*, *FAP*, *MMP-9*, and *VEGF* in fibroblasts. *In vivo*, sh-PDGF-D inhibited tumor growth, reduced the expressions of CD31, vimentin, α-SMA, FAP, MMP9, and VEGF, and promoted the expression of *E-cadherin*. **Conclusions**: Exosomes derived from HepG2 cells transfected with shPDGF-D prevent normal fibroblasts from transforming into CAFs, thus inhibiting angiogenesis and EMT of liver cancer.

Keywords: liver cancer; exosomes; cancer-associated fibroblasts; platelet-derived growth factor-D

1. Introduction

Liver cancer is one of the common tumors with the highest mortality at present [1]. The metastasis contributes to poor prognosis of patients with liver cancer, suggesting that early intervention for liver cancer metastasis is particularly important. It is found that the tumor microenvironment (TME) provides a good internal environment for the occurrence, development, and metastasis of liver cancer [2]. Fibroblasts are the classical supporting cell types, which were activated in response to the process of neoplasia. In the TME, the definition of cancer-associated fibroblasts (CAFs) can be simply viewed as fibroblasts that are located within a tumor [3]. The CAFs in TME can boost the invasion and metastasis of liver cancer cells by secreting cytokines and reconstructing the tumor microenvironment [4]. Although there are many sources of CAFs, including activated fibroblasts in the tumor microenvironment, bone marrow mesenchymal stem cells, adipose-derived mesenchymal stem cells, vascular smooth muscle cells, etc., CAFs can be identified by specific markers, such as α-*SMA* and *FAP* [4]. However, the mechanism by which liver cancer cells mediate the transformation of fibroblasts into CAFs is still unclear.

Exosomes are small vesicles secreted by cells with a diameter of 30–100 nm and wrapped by double lipid membranes [5]. They can regulate cell behavior by transmitting genetic information or functional proteins, so they are important mediators of communication between cells, such as tumor cells and CAFs [6]. CAFs are the main mesenchymal cells in TME and an important source of matrix metalloproteinases (MMPs), growth factors, chemokines, etc. [7]. It is found that stromal cells can receive exosomes from cancer cells, help cells to excrete cytotoxic drugs to induce drug resistance, regulate endothelial cell characteristics to promote angiogenesis and regulate epithelial-mesenchymal transition (EMT) to promote invasion and metastasis, thus creating a microenvironment to promote tumor growth [8]. It has been proven that tumor-derived exosomes can induce CAF activation and foster lung metastasis of liver cancer [9].

Platelet-derived growth factor (PDGF)-D belongs to the PDGFs family, which is overexpressed in multifarious cancers and participates in a series of cellular events, including proliferation, migration, invasion, blood vessel growth, etc. [10]. In addition, PDGF-D can also promote the proliferation and migration of fibroblasts [11]. Of note, Massimiliano Cadamuro *et al*. [12] found that cholangio-

carcinoma cells secrete PDGF-D to recruit liver myofibroblasts to promote tumor lymphangiogenesis in cholangiocarcinoma. This suggests that PDGF-D may play a certain role in mediating the transformation of normal fibroblasts into CAFs.

Therefore, in the current study, we sought to explore the role and mechanism of exosomes secreted by HepG2 cells transfected with PDGF-D specific short hairpin RNA (shPDGF-D) on the transformation of normal fibroblasts to CAFs.

2. Materials and Methods

2.1 Cell Culture

Human liver cancer cell line HepG2 (HB-8065, ATCC, Manassas, VA, USA) were cultured in DMEM (11965092, Thermo Fisher Scientific, Waltham, MA, USA) containing 10% Fetal Bovine Serum (FBS, 10091, Thermo Fisher, USA), 1% Penicillin-Streptomycin Solution (15140-122, Thermo Fisher, USA) in a humidified atmosphere with 5% CO_2 at 37 °C, and validated by short tandem repeat (STR) profiling and tested negative for mycoplasma contamination using MycoSensor PCR assay kit (Agilent, Hangzhou, China).

2.2 Cell Transfection

Human shPDGF-D (NM_025208.5, target sequence: 5′-ATCAAGAACGAACCAAATTAA-3′) lentiviral vector and its negative control (NC, target sequence: 5′-TTCTCCGAACGTGTCACGTCC-3′) were purchased from VectorBuilder (Guangzhou, China). In short, the vector was transfected into 293T cells with Lipofectamine™ 3000 (L3000150, Thermo Fisher, USA), and the transfection efficiency was assessed using a fluorescence microscope (BX53, Olympus, Tokyo, Japan) 24 hours after transfection. The cell supernatant was collected and filtered, and the filtered virus was then infected with HepG2 cells. After 48 hours, the expression of PDGF-D was detected by quantitative real-time polymerase chain reaction (qRT-PCR) and Western blotting.

2.3 qRT-PCR Assay

Briefly, total RNA was extracted by Trizol reagent (B511311, Sangon Biotech, Shanghai, China). Next, the PrimeScript RT reagent kit (Takara, Shiga, Japan) was used to synthesize the cDNA of each sample. The expression of *PDGF-D*, *α-SMA*, and *FAP* in cells was detected by a Real-Time PCR system (7500, ThermoFisher, USA) using Probe qPCR Mix (D7271, Beyotime, Shanghai, China). *GAPDH* was used as the internal reference. The relative expression levels were quantified by the $2^{-\Delta\Delta CT}$ approach. The sequences of the primers used are displayed in Table 1.

Table 1. Primers for quantitative real-time PCR (qRT-PCR) were used in this study.

Genes	Oligonucleotide sequences (5′ ∼ 3′)
PDGF-D	Forward 5′-GAGCAATCACCTCACAGACTTG-3′
	Reverse 5′-TTCCAGTTGACAGTTCCGCA-3′
α-SMA	Forward 5′-GGCATCCACGAAACCA-3′
	Reverse 5′-TTCCTGACCACTAGAGGGGG-3′
FAP	Forward 5′-GATTCATGGGCCTCCCAACA-3′
	Reverse 5′-CTAACCTCCTGAGCCCTCCT-3′
GAPDH	Forward 5′-GGCAAATTCAACGGCACAGT-3′
	Reverse 5′-TGAAGTCGCAGGAGACAACC-3′

PDGF-D: platelet-derived growth factor-D; *α-SMA*: alpha -smooth muscle actin; *FAP*: fibroblast activation protein; *GAPDH*: glyceraldehyde 3-phosphate dehydrogenase.

2.4 Western Blotting

Total protein was extracted using RIPA Lysis Solution (P0013K, Beyotime, China). The extracted protein has gone through the process of electrophoresis. After incubating with the primary antibody overnight at 4 °C, the membrane was washed with TBST buffer and incubated with the secondary antibody for 2 hours at room temperature. The protein bands were visualized by ECL Western Blotting Substrate (PE0010, Solarbio, Beiijng, China) and quantified using the Image J software (1.52v, NIH, Bethesda, MD, USA), with GAPDH serving as the internal control. The primary and secondary antibodies were as follows: PDGF-D (DF12690, 1:1000, Affinity, West Bridgford, UK); CD63 (1:1000, ab217345, Abcam, Fremont, CA, USA); CD81 (1:1000, ab109201, Abcam); CD9 (1:1000, ab92726, Abcam); α-SMA (1:1000, AF1032, Affinity), FAP (1:2000, AF0739, Affinity); matrix metallopeptidase-9 (MMP-9, AF5228, 1:2000, Affinity); vascular endothelial growth factor (VEGF) (1:1000, AF5131, Affinity); GAPDH (1:10,000, ab8245, Abcam); goat anti-rabbit antibody (1:5000, ab205718, Abcam); goat anti-mouse antibody (1:5000, ab6789, Abcam).

2.5 Exosome Extraction and Characterization

The separation of exosomes is described previously by sequential centrifugation [13]. In short, the HepG2 cells were cultured in a DMEM medium containing 10% exosomal-free FBS. After 48 hours, the supernatants from cells were centrifuged at 300 g for 10 minutes to discard cells, and then the supernatant was centrifuged at 16,500 g for 20 minutes to remove cell debris. The supernatant was filtrated using a 0.22 μm syringe filter and then centrifuged at 120,000 g (Beckman Type 90 Ti) for 70 minutes to precipitate exosomes. Finally, the exosome pellet was resuspended in PBS or lysis buffer before further analysis. In order to verify the exosomes, a nanoparticle tracking analysis (NTA, ZetaView PMX 120) was carried out to estimate the size distribution and nanoparticle concentration of the exosomes, the morphology of the exosomes was observed by using a transmission electron microscope (TEM, JEM-1400, JEOL, Akishima, Japan), and the specific markers of the exosomes (CD63, CD81 and CD9) were detected by western blot.

2.6 Isolation of Primary Fibroblasts

BALB/C mice (20–30 g) were acquired from Vital River (Beijing, China) and kept in a constant temperature (21 ± 0.5 °C) room with a natural circadian alternation and 50% humidity. After the mice were anesthetized with 1% sodium pentobarbital (50 mg/kg, P-010, Merck, German), the liver tissues of the mice were collected, cut into small pieces, and digested with type I collagenase (SCR103, Merck, German) at 37 °C for 2 hours. After centrifugation, the precipitate was resuspended with a complete medium and inoculated into 10 cm dishes.

All animal experiments were permitted by the Animal Experimentation Ethics Committee of Hangzhou Eyong Pharmaceutical Research and Development Center (Approval number: EYOUNG-20201030-02) and in accordance with the guidelines of the National Institutes of Health Laboratory Animal Care and Use Guidelines.

2.7 Co-Culture of Fibroblasts and Exosomes

The fibroblasts were placed in a 6-well plate at a density of 1×10^5 per well supplemented with 10% FBS-containing DMEM. After culturing for 24 hours, 50 µL of HepG2 shNC-exosome or HepG2 shPDGF-D-exosome medium with a concentration of 400 µg/µL was added to the 6-well plate for co-culture for 48 hours. For exosome uptake assays, the extracted exosomes were labeled using PKH67 (green) in line with the manufacturer's methods and co-cultured with fibroblasts at a concentration of 200 µg/mL for 48 h. Visualization of exosome uptake was observed using a laser scanning confocal microscope (LSM880, Zeiss, Jena, Germany).

2.8 Cell Counting Kit 8 (CCK8) Assay

Fibroblasts (2×10^3 per well) were added into 96-well plates, followed by the co-culture treatment with the exosomes (50 µg/mL) obtained from HepG2 with PDGF-D knockdown. After co-culture for 24, 48, 72, and 96 hours, 10 µL CCK-8 reagent (C0037, Beyotime, China) was added to each well and cultured for 2 h at 37 °C. The absorbance was measured by a microplate reader (ThermoFisher) at a wavelength of 450 nm.

2.9 EdU (5-Ethynyl-2′-Deoxyuridine) Incorporation Assay

The proliferating fibroblasts were determined by the EdU Kit (C0075, Beyotime, China). In short, the prepared EdU working solution was added to the above-mentioned 6-well plate for 48 hours of co-cultivation and incubated for 2 hours, then the culture solution was removed and 1 mL of fixing solution was added for fixation for 15 minutes. Then, after removing the fixing solution, cells were reacted with the permeating solution for 15 minutes and with a click reaction solution for 30 minutes. Then Hoechst 33342 solution was added to stain the nucleus. Finally, the results were observed under a fluorescence microscope (BX63, Olympus, Japan).

2.10 Immunofluorescence Assay

To detect the expression of E-cadherin, vimentin, α-SMA, and FAP, cells or tissues were fixed with 4% paraformaldehyde (E672002, Sangon, China), permeabilized with Triton-X-100 (A110694, Sangon), followed by blocking. Subsequently, cells were reacted with the primary antibody E-cadherin (1:100, ab231303, Abcam, UK), vimentin (1:200, ab92547, Abcam, UK), α-SMA (1:200, AF1032, Affinity, USA), FAP (1:200, AF0739, Affinity, USA) and CD31 (1:500, AF6191, Affinity, USA) overnight at 4 °C. The next day, cells were reacted with goat anti-rabbit antibody Alexa Fluor® 647 (ab150079, Abcam, UK) or Alexa Fluor® 488 (ab150077, Abcam, UK). The nucleus was stained with DAPI (E607303, Sangon) for 15 minutes. Finally, the images were captured using the fluorescence microscope and analyzed by using ImageJ software v2.0.0 (NIH, Bethesda, MD, USA).

2.11 Cell Cycle Test

Cell Cycle Kit (C1052, Beyotime, China) was used to detect the cell cycle. In short, the co-cultured cells were collected and centrifuged at 1000 g for 5 minutes. After removing the supernatant, the cells were resuspended with PBS (E607008, Sangon, China) and transferred to the centrifuge tube. Precooled 70% ethanol was added and incubated at 4 °C for 30 minutes. After washing, the configured propidium iodide (PI) staining solution was added and incubated in the dark for 30 minutes. Finally, the cell cycle was detected by flow cytometry.

2.12 Wound Healing Assays

A long scrape was created by a pipette, and PBS was used to remove detached cells on the surface. Afterward, the cells were incubated with DMEM in the incubator for 24 hours. The wounds were photographed at 0 and 48 hours by a microscope (BX53M, Olympus, Japan).

2.13 Xenograft Tumor Experiment

BALB/C nude mice (20–30 g) were also purchased from Vital River, and housed in a constant temperature (21 ± 0.5 °C) room with a natural circadian alternation and 50% humidity. Mice can eat and drink freely, and begin the experiment about 7 days after acclimatization. Nude mice were randomly divided into 2 groups, three in each group. Fibroblasts (2×10^6) co-cultured with HepG2 shNC-exosome or HepG2 shPDGF-D-exosome and HepG2 cells (3×10^6) were mixed in 200 µL PBS and then injected subcutaneously into mice. The volume of the subcutaneous tumor was measured with a caliper every three days and calculated using the formula: length $\times$ width^2/2. Four weeks later, the mice were euthanized by intraperitoneal injection of 250 mg/kg sodium pentobarbital [14]. The tumors were collected for follow-up immunofluorescence staining, qRT-PCR, and western blot.

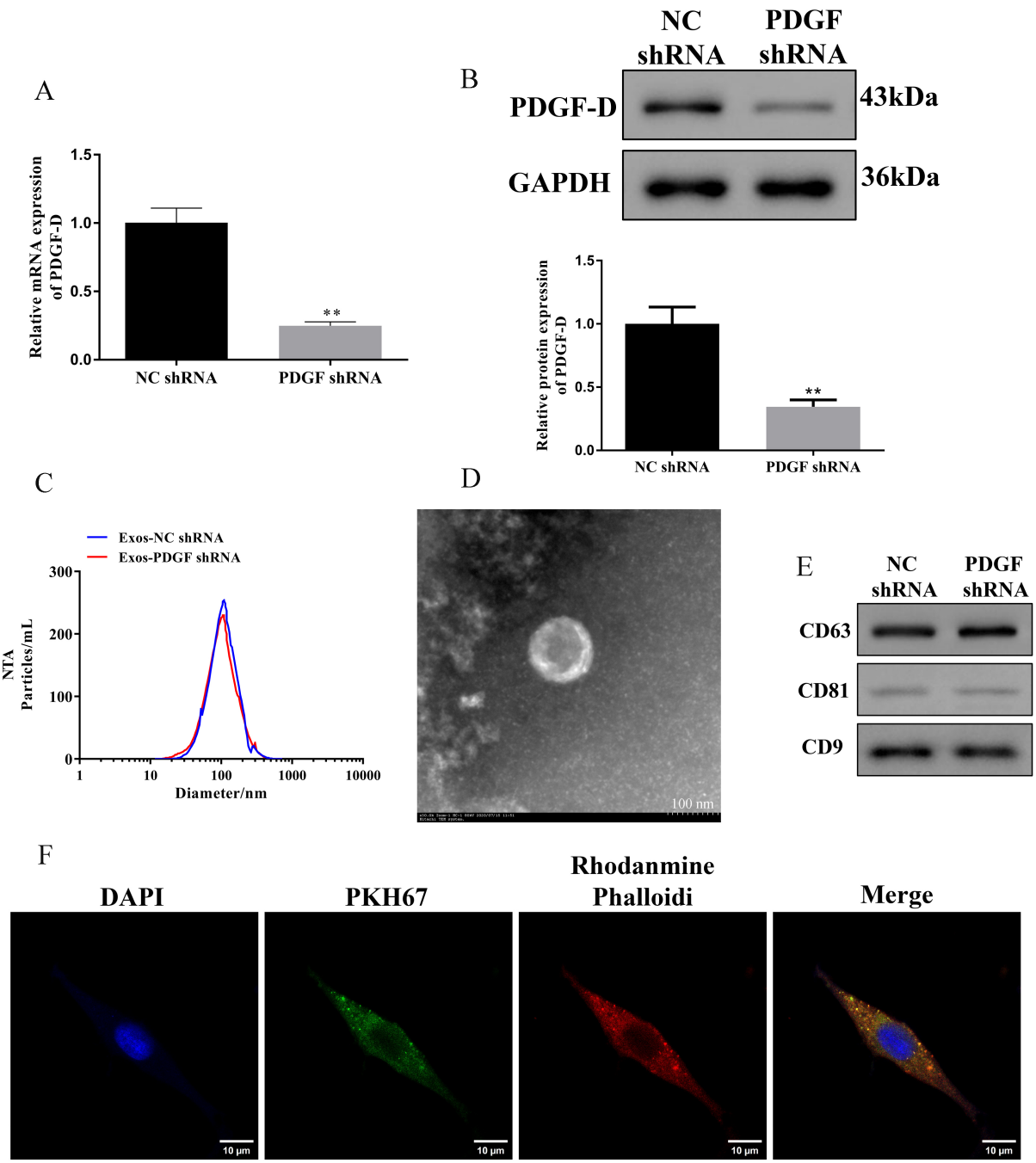

Fig. 1. Identification of exosomes in HepG2 cells with silencing of PDGF-D. (A,B) Relative expression of PDGF-D in HepG2 cells transfected with specific shRNAs against PDGF-D. Data are represented as mean ± SD (n = 3), $^{**}p < 0.01$, compared with the NC shRNA group. (C) nanoparticle size distribution. (D) Morphology of exosomes measured by transmission electron microscope (TEM). Scale bar, 100 nm. (E) Western blot was used to analyze the specific exosome surface markers (CD63, CD81, CD9). (F) A diagram of the uptake of exosomes in HepG2 cells with silencing of PDGF-D by fibroblasts. Scale bar, 10 μm.

2.14 Statistical Analysis

Statistical analysis was performed by GraphPad Prism 8.0 (GraphPad Software, Inc., San Diego, CA, USA). The results were expressed by mean ± standard deviation (SD). The comparisons between the two groups were analyzed using a student's *t*-test. Differences with $p < 0.05$ were considered statistically significant.

3. Results

3.1 Characterization of Exosomes Secreted by HepG2 Cells that Transfected with shPDGF-D

To evaluate the effect of PDGF-D, we transfected HepG2 cells with shPDGF-D, and the transfection efficiency was shown in Fig. 1A,B ($p < 0.01$). We determined the diameter and concentration of exosomes

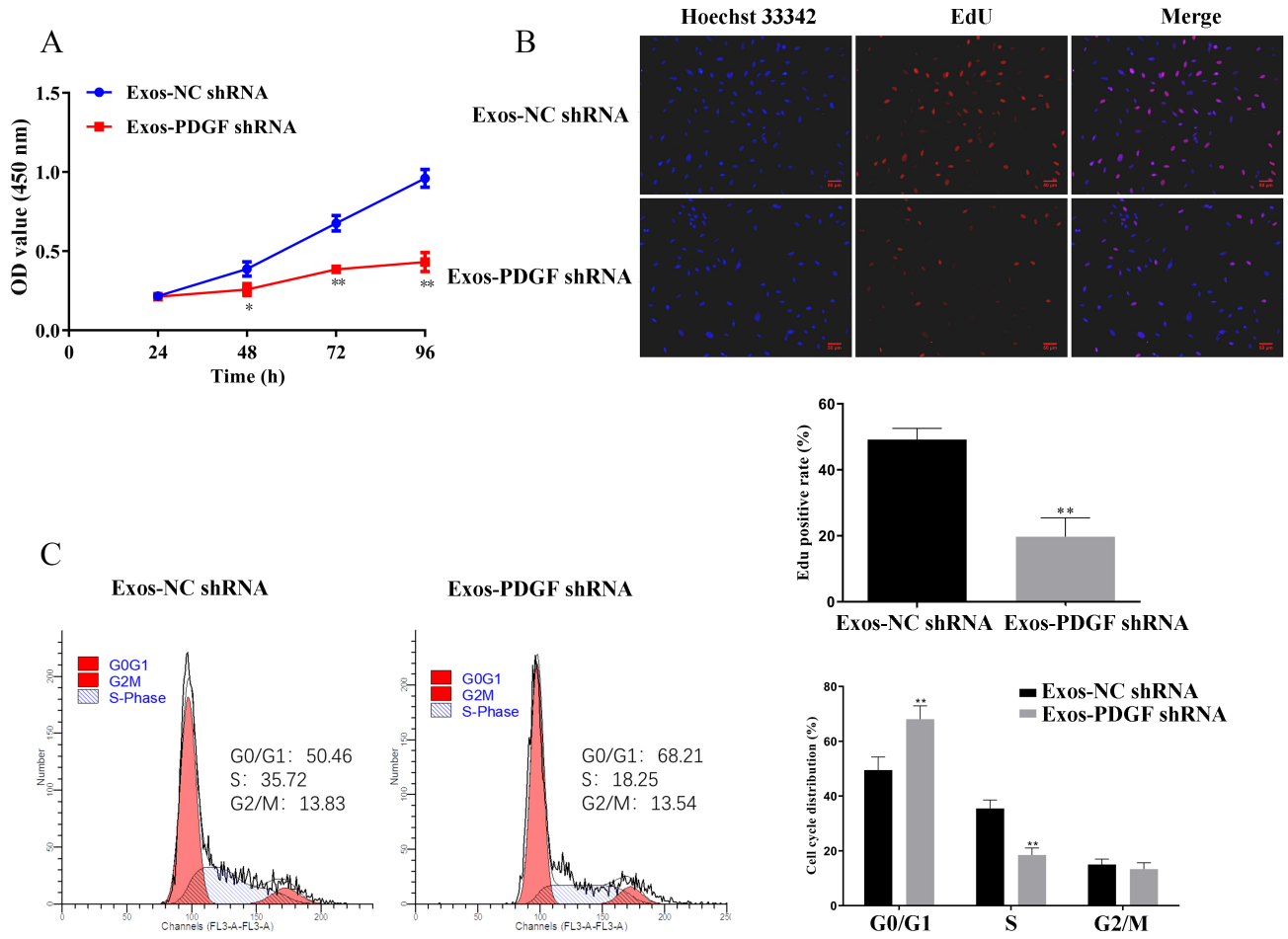

Fig. 2. Knockdown of PDGF-D in HepG2-derived exosomes inhibited the proliferation of fibroblasts. (A) Fibroblasts were incubated with exosomes in HepG2 cells with silencing of PDGF-D for 24, 48, 72, and 96 h, respectively. Cell viability was analyzed by cell counting kit-8 (CCK-8) assay. (B) EdU assays of Fibroblasts incubated with exosomes in HepG2 cells with silencing of PDGF-D were performed to evaluate cell proliferative ability. Scale bar, 50 μm. (C) Cell cycle distributions of fibroblasts in PDGF-D knockdown HepG2-derived exosomes were presented by flow cytometry. Results are represented as mean ± SD (n = 3). $*p < 0.05$, $**p < 0.01$ compared with Exos-NC shRNA group.

through nanoparticle tracking analysis (NTA) (Fig. 1C) and observed the morphology of exosomes through a TEM (Fig. 1D). The NTA showed that the peak diameter of exosomes was 110 nm (Fig. 1C). At the same time, the expression of characteristic proteins of exosomes (CD63, CD81, and CD9) was confirmed by western blot. Silencing PDGF-D did not affect the expression level of characteristic proteins of exosomes (Fig. 1E). The green fluorescence in exosomes was found in the perinuclear region of fibroblasts, suggesting that PKH67-labeled exosomes could enter into the cytoplasm of fibroblasts (Fig. 1F).

3.2 Regulation of the Biological Behavior of Fibroblasts by Exosomes Derived from HepG2 Cells Transfected with shPDGF-D

The exosomes of HepG2 cells with PDGF-D knockdown were co-cultured with mouse primary cultured fibroblasts, and the effects of exosomes derived from HepG2 cells on the biological behavior of fibroblasts were evaluated through a series of functional experiments. Compared with the Exos-NC shRNA group, exosomes derived from HepG2 cells transfected with shPDGF-D inhibited the cell viability and proliferation of fibroblasts (Fig. 2A,B, $p < 0.01$), induced the prolongation of the G0/G1 phase and the shortening of S phase (Fig. 2C, $p < 0.01$), and reduced the migration (Fig. 3A, $p < 0.01$).

3.3 Exosomes Derived from HepG2 Cells Transfected with shPDGF-D Prevented the Migration and Activation of Fibroblasts

The conversion of fibroblasts to CAFs is related to the EMT process, and activated fibroblasts have the ability to promote invasion and angiogenesis. Therefore, we evaluated the expression levels of EMT-related proteins, CAF markers, MMP-9, and VEGF. As shown in Fig. 3B, exosomes secreted by HepG2 cells transfected with shPDGF-

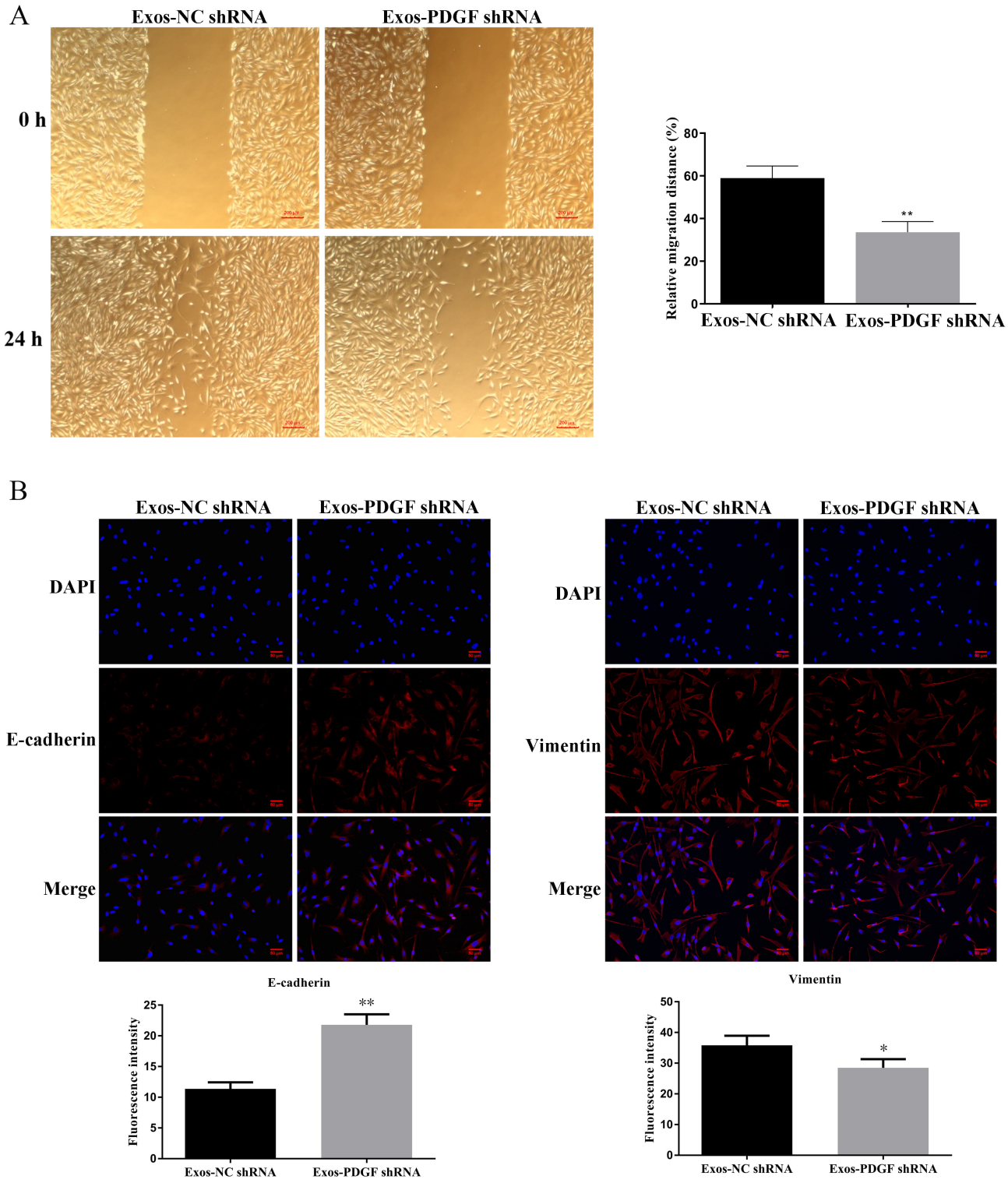

Fig. 3. Knockdown of PDGF-D in HepG2-derived exosomes inhibited the migration of fibroblasts. (A) Wound healing assays were performed in fibroblasts treated with exosomes in HepG2 cells with silencing of PDGF-D. Scale bar, 200 μm. (B) Immunofluorescent analysis for E-cadherin and Vimentin was detected in fibroblasts. Nuclei were stained blue (DAPI), and E-cadherin and Vimentin were stained red, Data are shown as mean ± SD (n = 3). Scale bar, 50 μm. *$p < 0.05$, **$p < 0.01$ compared with the Exos-NC shRNA group.

D could significantly increase the expression of E-cadherin in fibroblasts ($p < 0.01$), but inhibit the expression of vimentin ($p < 0.05$). We confirmed by qRT-PCR, western blot, and immunofluorescence that exosomes secreted by HepG2 cells transfected with shPDGF-D can reduce the expression levels of α-SMA and FAP in fibroblasts when

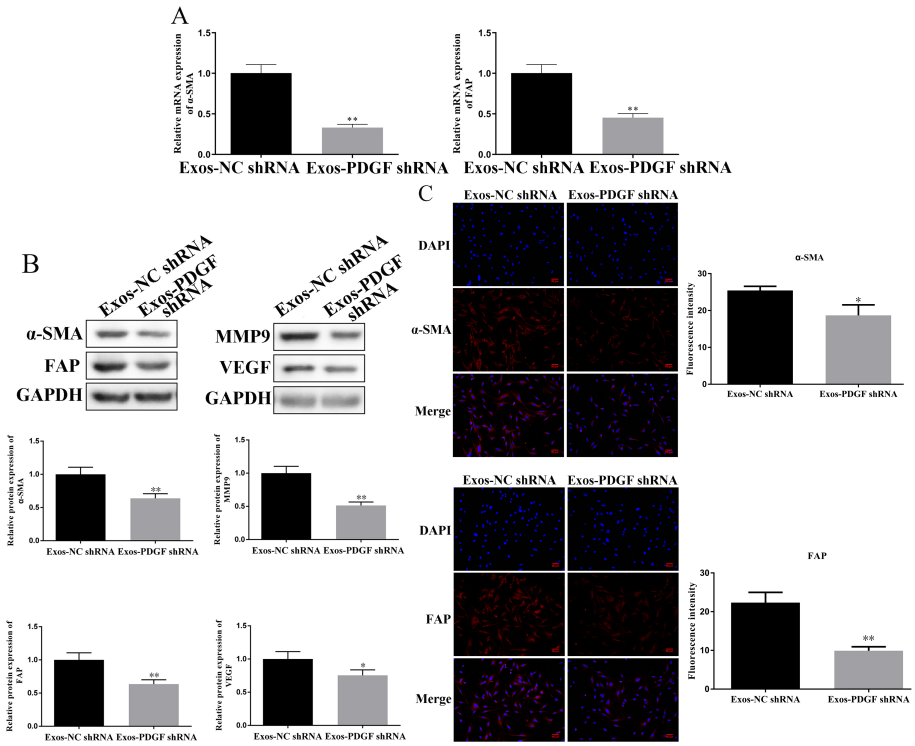

Fig. 4. Knockdown of PDGF-D in HepG2-derived exosomes regulates α-SMA, FAP, MMP 9, and VEGF expression in fibroblasts. (A) *α-SMA* and *FAP* expression levels were detected after being treated with exosomes in HepG2 cells with silencing of PDGF-D by real-time polymerase chain reaction (qRT-PCR). (B) Levels of the α-SMA, FAP, MMP 9, and VEGF protein in fibroblasts, as determined by Western blotting. (C) Immunofluorescence staining of α-SMA and FAP in fibroblasts treated with exosomes in HepG2 cells with silencing of PDGF-D. Scale bar: 50 μm. Data are shown as mean ± SD (n = 3). $*p < 0.05$, $**p < 0.01$ compared with the Exos-NC shRNA group. MMP, matrix metalloproteinases; VEGF, vascular endothelial growth factor.

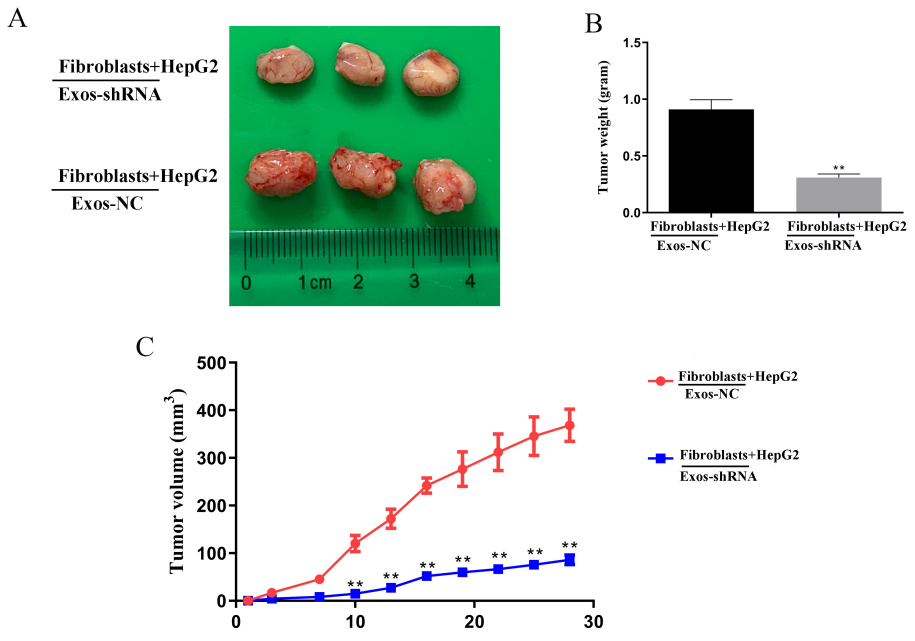

Fig. 5. Knockdown of PDGF-D in HepG2-derived exosomes suppresses the growth of Liver cancer tumor *in vivo*. (A) Representation images of tumor tissues of nude mice. Compared with the vector group, the (B) tumor weight and (C) volume significantly reduced in Knockdown of PDGF-D in HepG2-derived exosomes-treated fibroblasts and HepG2 cells in nude mice. Data are shown as mean ± SD (n = 3). $**p < 0.01$ compared with the Fibroblasts (Exos-NC)+Hepg2 group.

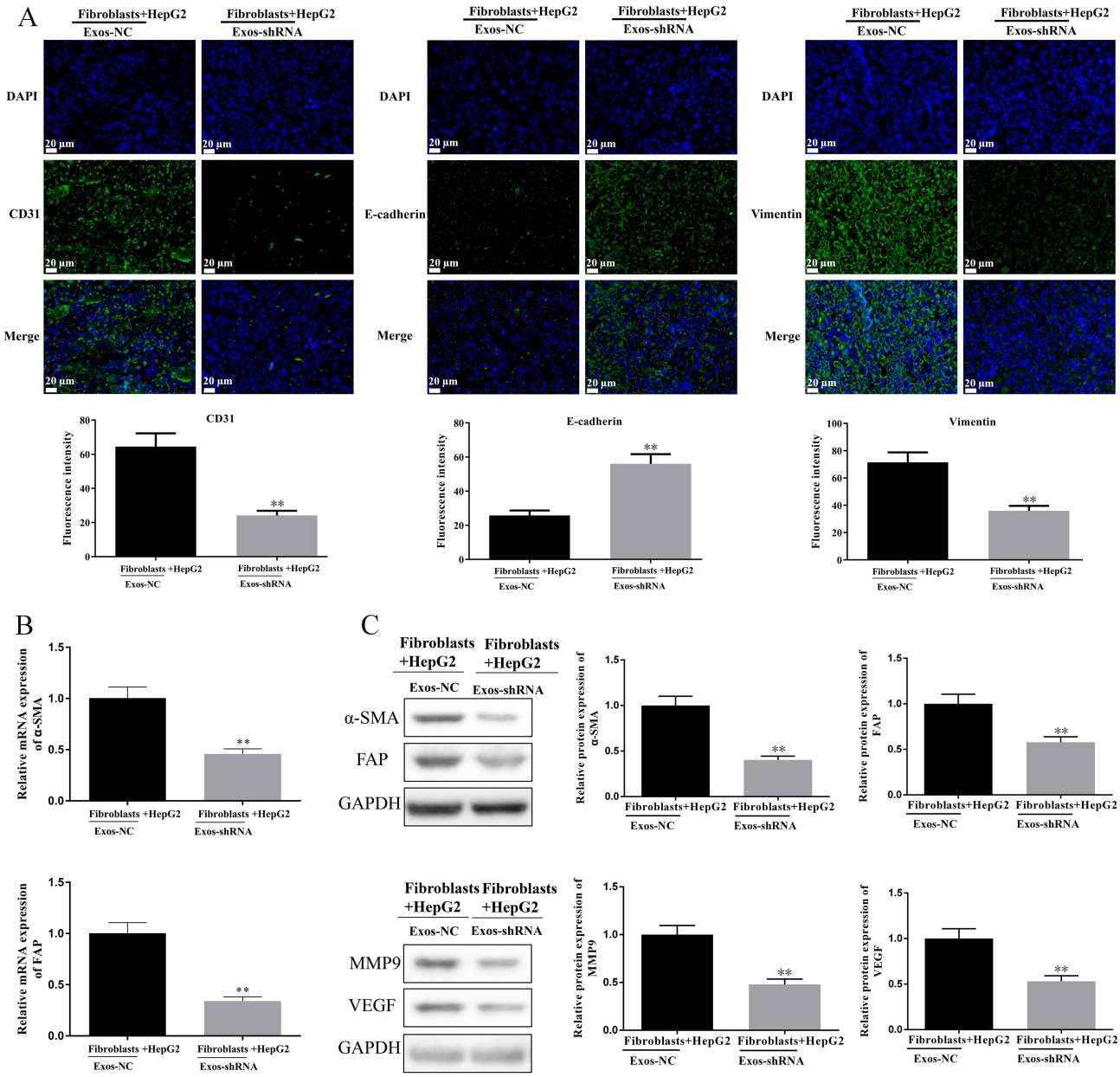

Fig. 6. Knockdown of PDGF-D in HepG2-derived exosomes regulates CD31, E-cadherin, Vimentin, α-SMA, FAP, MMP 9, and VEGF expression in tumor tissues. (A) Immunofluorescence staining of CD31, E-cadherin, and Vimentin in tumor tissues (magnification: ×400, scale bar = 20 μm). (B) α-SMA and FAP expression levels were detected in tumor tissues by qRT-PCR. (C) Levels of the α-SMA, FAP, MMP9, and VEGF protein in tumor tissues were detected by Western blotting. Data are shown as mean ± SD (n = 3). $^{**}p < 0.01$ compared with the Fibroblasts (Exos-NC)+Hepg2 group.

compared with the Exos-NC shRNA group (Fig. 4A–C, $p < 0.01$). In addition, the levels of MMP-9 and VEGF proteins were also inhibited by exosomes secreted by HepG2 cells transfected with shPDGF-D (Fig. 4B, $p < 0.05$).

3.4 ShPDGF-D Inhibited the Growth of Xenograft Tumors by Inhibiting the Activation of Fibroblasts

To further verify our conclusions, we carried out *in vivo* experiments. The results showed that compared with the Exos-NC group, the tumor size and volume of mice injected with HepG2 cells and fibroblasts (co-cultured with exosomes secreted by HepG2 cells transfected with shPDGF-D) were significantly reduced (Fig. 5A–C, $p < 0.01$). Not only that, fibroblasts (co-cultured with exosomes secreted by HepG2 cells transfected with shPDGF-D) reduced the expression of CD31, vimentin, α-SMA, FAP, MMP-9, and VEGF in tumor tissues, but elevated the levels of E-cadherin (Fig. 6A–C, $p < 0.01$).

4. Discussion

CAFs are mainly derived from activated normal fibroblasts and exhibit invasion and migration ability. Studies have shown that the activation process of normal fibroblasts mediated by tumor cells is closely related to exosomes [15]. Exosomes derived from tumor cells can not only reprogram normal fibroblasts into CAFs by transmitting miRNA but also induce normal fibroblasts to transform into CAFs by transmitting protein [16]. Ringuette *et al*. [17] found that the exosomes derived from bladder cancer cells carry transforming growth factor beta (TGF-β) to participate in the activation of SMAD signal, and then induce the activation of normal fibroblasts. In addition, there is evidence that fibroblasts activated by exosomes derived from metastatic cancer cells express more pro-angiogenic proteins, pro-proliferation proteins, and pro-invasion proteins than fibroblasts activated by exosomes derived from primary cancer cells [18]. This also further illustrates that metastatic cancer cells transmit functional proteins through exosomes, which activate fibroblasts into CAFs and obtain high invasion and invasion capabilities. In the previous study, CD63, CD81, and CD9 were used to distinguish exosomes and non-exosomal subgroups [19]. We followed this method and confirmed that transfection of shPDGF-D does not affect the characteristics of exosomes secreted by liver cancer cells.

PDGF-D can stimulate angiogenesis and extracellular matrix deposition, which is closely related to the development of cancer. It has been proved that PDGF-D has crosstalk with multiple signaling pathways such as cell survival and growth, EMT, invasion, angiogenesis, etc. [20]. Borkham-Kamphorst *et al*. [21] found that PDGF-D can activate hepatic stellate cells and myofibroblasts, thereby promoting liver fibrosis. It is worth noting that both hepatic stellate cells and myofibroblasts are sources of CAFs, and there has been evidence that PDGF-D enables hepatic myofibroblasts to promote tumor lymphangiogenesis in cholangiocarcinoma, which means blocking PDGF-D may be a way to hinder the cancer-promoting effect of CAFs [12]. Consistent with the previous studies, we found that exosomes shPDGF-D regulated the viability, proliferation, migration, and cell cycle of fibroblasts, thereby hindering the activation of fibroblasts.

Common downstream effectors of PDGF-D include EMT-associated proteins (E-cadherin, vimentin), MMP-9 and VEGF, etc. [20], and the activation of fibroblasts is also related to the occurrence of EMT [22]. The acquisition of invasiveness by liver cancer cells through the process of EMT is a key driver of the malignant progression of hepatocellular carcinoma [4,23]. EMT down-regulates the expression of the epithelial marker, E-cadherin, and up-regulates the expression of the mesenchymal epithelial marker, Vimentin, which results in the acquisition of a mesenchymal phenotype by the epithelial cells and confers on the hepatocellular carcinoma cells the ability to detach from the primary tumor site and metastasize to a distant location [23]. Therefore, the phenotype of hepatocellular carcinoma cells as epithelial or mesenchymal can be determined by the levels of E-cadherin and Vimentin, which can help to understand the degree of EMT of tumor cells. Additionally, MMP-9 is an important factor for cancer cell invasion. It has been found that down-regulation of PDGF-D in renal cell carcinoma cells and gastric cancer cells reduces the invasion and angiogenesis of cancer cells by inhibiting the expression of MMP-9 in cancer cells [24,25]. VEGF regulates the process of angiogenesis, and it has been shown that down-regulation of PDGF-D inhibits the expression of VEGF in gastric cancer cells and thus affects the development of gastric cancer [25]. In addition, Fan *et al*. [26] reported that exosomes derived from lung cancer cells increased the expression of VEGF and MMP-9, thereby promoting the transformation of fibroblasts to CAFs. These evidences showed that PDGF-D can promote the transformation of fibroblasts into CAFs by regulating the expression of E-cadherin, vimentin, MMP9 and VEGF, which is consistent with our research results. Moreover, the decrease of α-SMA and FAP expression meant that exosome shPDGF-D inhibits the transformation of fibroblasts into CAFs.

Tumor cells stimulate fibroblasts to transform into CAFs by secreting exosomes, while CAFs secrete cytokines like MMP and TGF-β and induce EMT in cancer cells, so as to promote the development of tumors [27]. Liu *et al*. [28] found that CAFs promoted the metastasis of hepatocellular carcinoma by secreting chemokines to activate the TGF-β pathway. Jia *et al*. [29] reported that CAFs induced EMT of liver cancer via the Interleukin 6 (IL-6)/STAT3 axis. However, Yamanaka *et al*. [30] believe that inhibiting the activation of fibroblasts can hinder the promotion of CAFs in intrahepatic cholangiocarcinoma. In our *in vivo* experiment, shPDGF-D inhibited tumor growth by inhibiting fibroblast activation. Furthermore, after PDGF-D was silenced, angiogenesis-related proteins (CD31, VEGF), vimentin, CAFs markers and MMP9 in tumor tissues were down-regulated, while E-cadherin was up-regulated, which on the one hand verified that the activation of fibroblasts was blocked, on the other hand, indicated that the EMT and angiogenesis ability of tumor decreased.

Studies have shown that cardiotrophin-like cytokine factor 1 (CLCF1), which is derived from CAFs in liver cancer, causes cancer cells to secrete more chemokine ligand 6 (CXCL6) and TGF-β. CXCL6 promotes cancer progression by activating PI3K/Akt or NF-κB signaling [31,32]. Follistatin-like protein 1 (FSTL1) is a pro-inflammatory factor mainly secreted by CAFs. FSTL1 binds to the TLR4 receptor on liver cancer cells and promotes cancer stemness by affecting the AKT/mTOR/4EBP1 signaling pathway [33]. Another study showed that exosomes secreted by CAFs release TUG1, which promotes glycolysis in liver cancer cells through the miR-524-5p/SIX1 axis [34]. In this study, the results showed that the shPDGF-D exosomes

significantly inhibited fibroblast transformation into CAFs. However, there are some shortcomings in this study. It would be beneficial to provide more detail on how shPDGF-D exosomes specifically impact EMT-related pathways. The role of other PDGF-D-related target genes and the clinical implications of the exosomes from shPDGF-D HeapG2 cells needed further investigation.

5. Conclusions

In summary, our research proves that exosomes derived from HepG2 cells transfected with shPDGF-2 prevent normal fibroblasts from transforming into CAFs, thus inhibiting angiogenesis and EMT of liver cancer.

Availability of Data and Materials

The data set used and analyzed in this study can be obtained from the corresponding author upon reasonable request.

Author Contributions

JCX contributed the design of the study. YYW and LSYY contributed to perform *in vitro* and *in vivo* experiments and write article. YYW and HYZ contributed to analyze experiment data. All authors contributed to editorial changes in the manuscript. All authors read and approved the final manuscript. All authors have participated sufficiently in the work and agreed to be accountable for all aspects of the work.

Ethics Approval and Consent to Participate

The manuscript was approved by the Committee on Experimental Animals of Hangzhou Eyong Pharmaceutical Research and Development Center (Approval number: EYOUNG-20201030-02) and was in accordance with the National Institutes of Health Laboratory Animal Care and Use Guidelines.

Acknowledgment

Not applicable.

Funding

This research received no external funding.

Conflict of Interest

The authors declare no conflict of interest.

References

[1] Anwanwan D, Singh SK, Singh S, Saikam V, Singh R. Challenges in liver cancer and possible treatment approaches. Biochimica et Biophysica Acta. Reviews on Cancer. 2020; 1873: 188314. https://doi.org/10.1016/j.bbcan.2019.188314.

[2] Affo S, Yu LX, Schwabe RF. The Role of Cancer-Associated Fibroblasts and Fibrosis in Liver Cancer. Annual Review of Pathology. 2017; 12: 153–186. https://doi.org/10.1146/annurev-pathol-052016-100322.

[3] Chen Y, McAndrews KM, Kalluri R. Clinical and therapeutic relevance of cancer-associated fibroblasts. Nature Reviews. Clinical Oncology. 2021; 18: 792–804. https://doi.org/10.1038/s41571-021-00546-5.

[4] Baglieri J, Brenner DA, Kisseleva T. The Role of Fibrosis and Liver-Associated Fibroblasts in the Pathogenesis of Hepatocellular Carcinoma. International Journal of Molecular Sciences. 2019; 20: 1723. https://doi.org/10.3390/ijms20071723.

[5] Milane L, Singh A, Mattheolabakis G, Suresh M, Amiji MM. Exosome mediated communication within the tumor microenvironment. Journal of Controlled Release. 2015; 219: 278–294. https://doi.org/10.1016/j.jconrel.2015.06.029.

[6] Wortzel I, Dror S, Kenific CM, Lyden D. Exosome-Mediated Metastasis: Communication from a Distance. Developmental Cell. 2019; 49: 347–360. https://doi.org/10.1016/j.devcel.2019.04.011.

[7] Micke P, Ostman A. Exploring the tumour environment: cancer-associated fibroblasts as targets in cancer therapy. Expert Opinion on Therapeutic Targets. 2005; 9: 1217–1233. https://doi.org/10.1517/14728222.9.6.1217.

[8] Zhang L, Yu D. Exosomes in cancer development, metastasis, and immunity. Biochimica et Biophysica Acta. Reviews on Cancer. 2019; 1871: 455–468. https://doi.org/10.1016/j.bbcan.2019.04.004.

[9] Fang T, Lv H, Lv G, Li T, Wang C, Han Q, *et al*. Tumor-derived exosomal miR-1247-3p induces cancer-associated fibroblast activation to foster lung metastasis of liver cancer. Nature Communications. 2018; 9: 191. https://doi.org/10.1038/s41467-017-02583-0.

[10] Wu Q, Hou X, Xia J, Qian X, Miele L, Sarkar FH, *et al*. Emerging roles of PDGF-D in EMT progression during tumorigenesis. Cancer Treatment Reviews. 2013; 39: 640–646. https://doi.org/10.1016/j.ctrv.2012.11.006.

[11] Folestad E, Kunath A, Wågsäter D. PDGF-C and PDGF-D signaling in vascular diseases and animal models. Molecular Aspects of Medicine. 2018; 62: 1–11. https://doi.org/10.1016/j.mam.2018.01.005.

[12] Cadamuro M, Brivio S, Mertens J, Vismara M, Moncsek A, Milani C, *et al*. Platelet-derived growth factor-D enables liver myofibroblasts to promote tumor lymphangiogenesis in cholangiocarcinoma. Journal of Hepatology. 2019; 70: 700–709. https://doi.org/10.1016/j.jhep.2018.12.004.

[13] Lässer C, Eldh M, Lötvall J. Isolation and characterization of RNA-containing exosomes. Journal of Visualized Experiments: JoVE. 2012; e3037. https://doi.org/10.3791/3037.

[14] Dutton JW, 3rd, Artwohl JE, Huang X, Fortman JD. Assessment of Pain Associated with the Injection of Sodium Pentobarbital in Laboratory Mice (*Mus musculus*). Journal of the American Association for Laboratory Animal Science. 2019; 58: 373–379. https://doi.org/10.30802/AALAS-JAALAS-18-000094.

[15] Zhou Y, Ren H, Dai B, Li J, Shang L, Huang J, *et al*. Hepatocellular carcinoma-derived exosomal miRNA-21 contributes to tumor progression by converting hepatocyte stellate cells to cancer-associated fibroblasts. Journal of Experimental & Clinical Cancer Research. 2018; 37: 324. https://doi.org/10.1186/s13046-018-0965-2.

[16] Yang X, Li Y, Zou L, Zhu Z. Role of Exosomes in Crosstalk Between Cancer-Associated Fibroblasts and Cancer Cells. Frontiers in Oncology. 2019; 9: 356. https://doi.org/10.3389/fonc.2019.00356.

[17] Ringuette Goulet C, Bernard G, Tremblay S, Chabaud S, Bolduc S, Pouliot F. Exosomes Induce Fibroblast Differentiation into Cancer-Associated Fibroblasts through TGFβ Signaling. Molecular Cancer Research. 2018; 16: 1196–1204. https://doi.org/10.1158/1541-7786.MCR-17-0784.

[18] Rai A, Greening DW, Chen M, Xu R, Ji H, Simpson RJ. Exosomes Derived from Human Primary and Metastatic Colorectal Cancer Cells Contribute to Functional Heterogeneity of Activated Fibroblasts by Reprogramming Their Proteome. Proteomics. 2019; 19: e1800148. https://doi.org/10.1002/pmic.201800148.

[19] Kowal J, Arras G, Colombo M, Jouve M, Morath JP, Primdal-Bengtson B, *et al*. Proteomic comparison defines novel markers to characterize heterogeneous populations of extracellular vesicle subtypes. Proceedings of the National Academy of Sciences of the United States of America. 2016; 113: E968–E977. https://doi.org/10.1073/pnas.1521230113.

[20] Wang Z, Ahmad A, Li Y, Kong D, Azmi AS, Banerjee S, *et al*. Emerging roles of PDGF-D signaling pathway in tumor development and progression. Biochimica et Biophysica Acta. 2010; 1806: 122–130. https://doi.org/10.1016/j.bbcan.2010.04.003.

[21] Borkham-Kamphorst E, van Roeyen CRC, Ostendorf T, Floege J, Gressner AM, Weiskirchen R. Pro-fibrogenic potential of PDGF-D in liver fibrosis. Journal of Hepatology. 2007; 46: 1064–1074. https://doi.org/10.1016/j.jhep.2007.01.029.

[22] Lau EYT, Lo J, Cheng BYL, Ma MKF, Lee JMF, Ng JKY, *et al*. Cancer-Associated Fibroblasts Regulate Tumor-Initiating Cell Plasticity in Hepatocellular Carcinoma through c-Met/FRA1/HEY1 Signaling. Cell Reports. 2016; 15: 1175–1189. https://doi.org/10.1016/j.celrep.2016.04.019.

[23] Sengez B, Carr BI, Alotaibi H. EMT and Inflammation: Crossroads in HCC. Journal of Gastrointestinal Cancer. 2023; 54: 204–212. https://doi.org/10.1007/s12029-021-00801-z.

[24] Xu L, Tong R, Cochran DM, Jain RK. Blocking platelet-derived growth factor-D/platelet-derived growth factor receptor beta signaling inhibits human renal cell carcinoma progression in an orthotopic mouse model. Cancer Research. 2005; 65: 5711–5719. https://doi.org/10.1158/0008-5472.CAN-04-4313.

[25] Zhao L, Zhang C, Liao G, Long J. RNAi-mediated inhibition of PDGF-D leads to decreased cell growth, invasion and angiogenesis in the SGC-7901 gastric cancer xenograft model. Cancer Biology & Therapy. 2010; 9: 42–48. https://doi.org/10.4161/cbt.9.1.10282.

[26] Fan J, Xu G, Chang Z, Zhu L, Yao J. miR-210 transferred by lung cancer cell-derived exosomes may act as proangiogenic factor in cancer-associated fibroblasts by modulating JAK2/STAT3 pathway. Clinical Science. 2020; 134: 807–825. https://doi.org/10.1042/CS20200039.

[27] Fiori ME, Di Franco S, Villanova L, Bianca P, Stassi G, De Maria R. Cancer-associated fibroblasts as abettors of tumor progression at the crossroads of EMT and therapy resistance. Molecular Cancer. 2019; 18: 70. https://doi.org/10.1186/s12943-019-0994-2.

[28] Liu J, Chen S, Wang W, Ning BF, Chen F, Shen W, *et al*. Cancer-associated fibroblasts promote hepatocellular carcinoma metastasis through chemokine-activated hedgehog and TGF-β pathways. Cancer Letters. 2016; 379: 49–59. https://doi.org/10.1016/j.canlet.2016.05.022.

[29] Jia C, Wang G, Wang T, Fu B, Zhang Y, Huang L, *et al*. Cancer-associated Fibroblasts induce epithelial-mesenchymal transition *via* the Transglutaminase 2-dependent IL-6/IL6R/STAT3 axis in Hepatocellular Carcinoma. International Journal of Biological Sciences. 2020; 16: 2542–2558. https://doi.org/10.7150/ijbs.45446.

[30] Yamanaka T, Harimoto N, Yokobori T, Muranushi R, Hoshino K, Hagiwara K, *et al*. Nintedanib inhibits intrahepatic cholangiocarcinoma aggressiveness via suppression of cytokines extracted from activated cancer-associated fibroblasts. British Journal of Cancer. 2020; 122: 986–994. https://doi.org/10.1038/s41416-020-0744-7.

[31] Song M, He J, Pan QZ, Yang J, Zhao J, Zhang YJ, *et al*. Cancer-Associated Fibroblast-Mediated Cellular Crosstalk Supports Hepatocellular Carcinoma Progression. Hepatology. 2021; 73: 1717–1735. https://doi.org/10.1002/hep.31792.

[32] Zhang Z, Tan X, Luo J, Yao H, Si Z, Tong JS. The miR-30a-5p/CLCF1 axis regulates sorafenib resistance and aerobic glycolysis in hepatocellular carcinoma. Cell Death & Disease. 2020; 11: 902. https://doi.org/10.1038/s41419-020-03123-3.

[33] Loh JJ, Li TW, Zhou L, Wong TL, Liu X, Ma VWS, *et al*. FSTL1 Secreted by Activated Fibroblasts Promotes Hepatocellular Carcinoma Metastasis and Stemness. Cancer Research. 2021; 81: 5692–5705. https://doi.org/10.1158/0008-5472.CAN-20-4226.

[34] Lu L, Huang J, Mo J, Da X, Li Q, Fan M, *et al*. Exosomal lncRNA TUG1 from cancer-associated fibroblasts promotes liver cancer cell migration, invasion, and glycolysis by regulating the miR-524-5p/SIX1 axis. Cellular & Molecular Biology Letters. 2022; 27: 17. https://doi.org/10.1186/s11658-022-00309-9.